
This is an electronic reprint of the original article.
This reprint may differ from the original in pagination and typographic detail.

Author(s): Braskén, M. & Lindberg, M. & Sopenan, M. & Lipsanen, Harri & Tulkki, J.

Title: Temperature dependence of carrier relaxation in strain-induced quantum dots

Year: 1998

Version: Final published version

Please cite the original version:

Braskén, M. & Lindberg, M. & Sopenan, M. & Lipsanen, Harri & Tulkki, J.. 1998. Temperature dependence of carrier relaxation in strain-induced quantum dots. *Physical Review B*. Volume 58, Issue 24. P. R15993-R15996. ISSN 1098-0121 (printed). DOI: 10.1103/physrevb.58.r15993.

Rights: © 1998 American Physical Society (APS). <http://www.aps.org/>

All material supplied via Aaltodoc is protected by copyright and other intellectual property rights, and duplication or sale of all or part of any of the repository collections is not permitted, except that material may be duplicated by you for your research use or educational purposes in electronic or print form. You must obtain permission for any other use. Electronic or print copies may not be offered, whether for sale or otherwise to anyone who is not an authorised user.

Temperature dependence of carrier relaxation in strain-induced quantum dots

M. Braskén and M. Lindberg

Department of Physics, Åbo Akademi University, FIN-20500 Turku, Finland

M. Sopanen and H. Lipsanen

Optoelectronics Laboratory, Helsinki University of Technology, FIN-02015 HUT, Finland

J. Tulkki

Laboratory of Computational Engineering, Helsinki University of Technology, FIN-02015 HUT, Finland

(Received 27 August 1998)

We report experimental observation and theoretical interpretation of temperature-dependent, time-resolved luminescence from strain-induced quantum dots. The experimental results are well described by a master equation model for the electrons. The intraband relaxation in the conduction band and the radiative recombination rate are governed by the hole populations resulting in prominent temperature dependence of the relaxation process. Even when only a few electrons and holes are confined in a single quantum dot the Auger-like process provides a rapid intraband relaxation channel for electrons that can replace the phonon scattering as the dominant relaxation mechanism. [S0163-1829(98)51148-4]

The temperature dependence of the carrier relaxation is critical in developing optoelectronic components based on semiconductor quantum dots (QD's). In bulk and in quantum wells (QW's) the dominant mechanism of carrier relaxation is LO-phonon emission. Due to the discreteness of the energy levels, however, this is no longer an efficient relaxation process in QD's and the intralevel relaxation has been assumed to proceed by the slower LA-phonon emission process.¹ This slowing down of the carrier relaxation in QD's has been called a phonon bottleneck.² A conclusive, experimental verification of the existence of this phonon bottleneck is, however, at the moment lacking. Relaxation rates that are much faster,³⁻⁵ and slower,⁶ than the calculated LA-phonon rates have been reported. Suggestions for mechanisms that would break the bottleneck, extend from Coulomb scattering in the dense electron-hole plasma created by the excitation,⁷ Auger-like energy transfer between electrons and holes,⁸ to multiphonon processes involving defects.⁹ A reason for this controversy is that the experiments have been done on different types of QD samples and that the inhomogeneous broadening of the QD luminescence lines limits the knowledge of the energy level structure. The presence of surface states, defects and impurities may also further complicate the picture. In this paper we present both experimental and theoretical results of the temperature dependence of luminescence in strain-induced QD's. QD's induced by an InP stressor on an $\text{In}_x\text{Ga}_{1-x}\text{As}/\text{GaAs}$ QW (Refs. 10 and 11) provide, due to their size homogeneity and lack of dislocations, surface states and impurities, an excellent QD system for a detailed study of carrier relaxation.

Our QD sample was grown by metal-organic vapor phase epitaxy at 650 °C.¹⁰ The sample consists of a 7-nm-thick $\text{In}_{0.10}\text{Ga}_{0.90}\text{As}/\text{GaAs}$ QW separated by a 5-nm-thick GaAs top barrier from the surface. To complete the strain-induced QD structure, self-organized InP islands, which act as stressors, were subsequently grown onto the GaAs surface by depositing 3 monolayers of InP. The islands are about 75 nm

wide and 22–24 nm high with a density of $\approx 10^9 \text{ cm}^{-2}$. The strain field below the InP island produces a nearly parabolic QD potential for both electrons and holes, as indicated by both optical measurements¹² and calculations.¹¹ The optical measurements were performed using 200-fs pulses from a 76-MHz mode locked titanium-sapphire laser operating at 800 nm. The light was focused onto a spot with a diameter of 100 μm . The sample was mounted in a variable-temperature closed-cycle cryostat operating down to 12 K. Time-resolved luminescence was spectrally resolved using a 0.5-m monochromator and detected by a single-photon-counting technique using a cooled microchannel plate photomultiplier tube. The temporal resolution was about 35 ps. Figure 1 shows the experimental time-resolved luminescence spectra measured at $T=12 \text{ K}$, 30 K, and 50 K. The pump intensity of

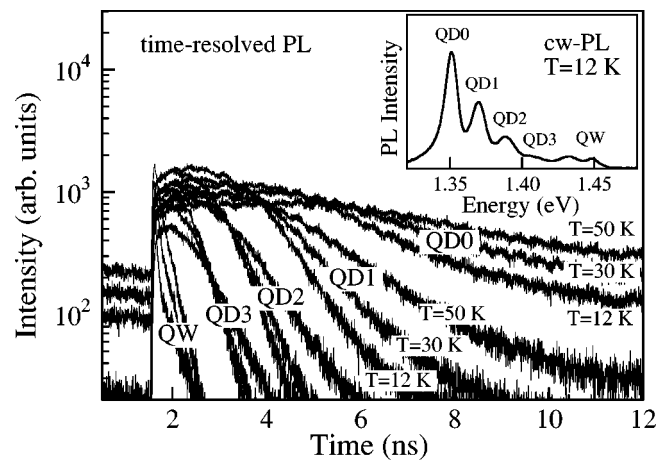


FIG. 1. The time-resolved photoluminescence from strain-induced QD's at temperatures of 12, 30, and 50 K. The figure shows the luminescence intensities of the four lowest QD transitions and the QW $\text{C1} \rightarrow \text{HH1}$ transition. The inset shows the cw luminescence at 12 K.

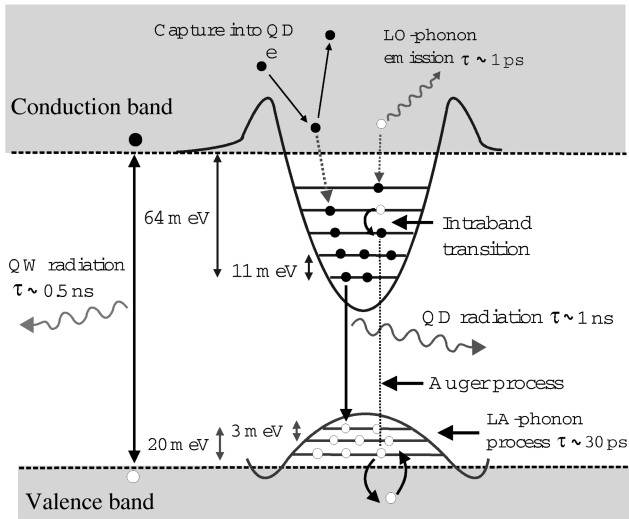


FIG. 2. A schematic picture of the different mechanisms involved in the carrier relaxation.

40 W/cm^{-2} was chosen so that the ground and excited QD states were at least partly filled. The inset shows the time-averaged luminescence curve recorded at 12 K. The ground-state QD transition at 1.35 eV is indexed by QD0, first excited state by QD1, etc. The transition at 1.45 eV arises from the unperturbed QW between the stressor islands. The initial rise time for all transitions of the time-resolved spectra is faster than the resolution of the detection. However, a rise time of ≈ 1 ps has been obtained from a similar sample using a luminescence up-conversion measurement.¹³ After the initial rise, the intensity from the QD0 transition stays almost constant for several ns while the QW and the excited-state transitions start to decay beginning from the highest energy transitions. As the temperature is increased, the QW transition decays more rapidly, while for all QD transitions the decay time becomes slower.

The depth of the confinement potential is approximately 100 meV for the electrons, and 30 meV for the holes.¹¹ For the lowest laying states the level spacing is 11 meV between consecutive electron states, while for the holes it is 3–4 meV (see Fig. 2). Due to the shallower potential well and smaller level spacing the holes are captured into the QD from the QW faster than the electrons. The capture is mediated by Coulomb scattering and LO-phonon emission ($E_{lo}^{GaAs} = 35$ meV). The rate of both of these processes depends on the carrier density in the QW, and the capture process becomes inefficient at low carrier densities in the QW.¹⁴ When the electrons and holes are in the QD they can recombine radiatively, on a time scale of ≤ 1 ns, and/or undergo an intraband transition. Two candidates for the intraband relaxation mechanism are Coulomb scattering and LA-phonon emission (the sharp, discrete states makes the LO-phonon process unlikely). For the electrons the bulk LA phonons are much too slow ($\tau_{la}^e \approx 10^3$ ns) to make a contribution before the electrons and holes recombine radiatively.¹⁴ However, the level spacing in the valence band is smaller and therefore the hole LA-phonon rate will be much faster ($\tau_{la}^h = 33$ ps for a level spacing of 3 meV). The Coulomb mediated intraband scattering mechanism described by Bockelmann and Egeler⁷ is very efficient in the first 0.5 ns of the carrier relaxation, when

the carrier density in the QW is high, but after that it becomes too slow to contribute to the relaxation.¹⁴ A Coulomb process that does not need carriers in the QW to proceed is introduced below.

To calculate the time-dependent QD luminescence, we need the electron and hole population in the QD as a function of time. For the electrons the populations are obtained by solving a master equation.¹⁵ The master equation gives the probability $w(\mu; \lambda)$ for finding the electron system in the many-particle state μ , and the hole system in the many-particle state λ . We neglect the Coulomb interaction between the carriers in calculating the eigenstates. The many-particle states will thus be product states of single-particle electron and hole states. We factorize the probability: $w(\mu; \lambda) = u^e(\mu)u^h(\lambda)$, where $u^e(\mu)$ and $u^h(\lambda)$ are the probabilities of finding the electron and hole system in states μ and λ , respectively, and then sum over the hole degrees of freedom. Normalizing the probabilities $\sum_{\lambda} u^h(\lambda) = 1$ and introducing the notation $\Gamma_{\mu \rightarrow \mu'} = \sum_{\lambda} \Gamma_{\mu \lambda \rightarrow \mu' \lambda}$, $\Gamma_{\mu \lambda \rightarrow \mu' \lambda'}$, where $\Gamma_{\mu \lambda \rightarrow \mu' \lambda'}$ is the rate from state $(\mu \lambda)$ to $(\mu' \lambda')$, we obtain the master equation for the electron system

$$\dot{u}^e(\mu) = - \sum_{\mu'} \Gamma_{\mu \rightarrow \mu'} u^e(\mu) + \sum_{\mu'} \Gamma_{\mu' \rightarrow \mu} u^e(\mu') \quad (1)$$

The rates $\Gamma_{\mu \rightarrow \mu'}$ of the processes that changes the many-electron state from μ to μ' , are described below. Our aim has been to find one set of relaxation parameters that fit all temperatures. Equation (1) contains all intraband relaxation processes, and the radiative recombination rate that is proportional to the measured luminescence.

The carrier capture from the QW is described using a phenomenological pumping rate $\Gamma_p(t) = \Gamma_0 e^{-t/\tau_0}$, where the value of Γ_0 depends on the initial carrier density in the QW, and thus on the intensity of the excitation pulse. The time dependence of the pump rate reflects the decrease in the number of carriers in the QW, due to radiative recombination and/or capture into the QD (the measured decay time of the QW luminescence is of the order of 0.5 ns). The time scale on which there is a significant pumping is given by τ_0 in our model. The electron intralevel transitions, at low QW carrier densities, is taken to proceed by a mechanism where the transition of an electron to a lower level is followed by the subsequent emission of a hole from the QD (Ref. 8) (processes in which a hole is captured and an electron is excited or an electron is deexcited while another is excited in the QD have both negligible rates). This Auger rate depends on the hole population f_h^j , where j refers to any hole level that is close enough to the QW continuum states, so that the energy difference between the initial and final electron level is enough to eject the hole into the QW continuum. The rate for the process where an electron makes a transition from level i to f while the hole is ejected from level j into the continuum state \mathbf{k}_f , is obtained from the Fermi's golden rule expression

$$\Gamma_{ij \rightarrow f \mathbf{k}_f}^A = \frac{2\pi}{\hbar} \sum_{\mathbf{k}} |\langle \phi_f^e; \phi_h(\mathbf{k}) | V(\mathbf{r}_e - \mathbf{r}_h) | \phi_i^e; \phi_h^j \rangle|^2 \times f_h^j \delta(\Delta \epsilon_{if} - \epsilon(\mathbf{k})) \quad (2)$$

where V is the Coulomb potential and $\Delta \epsilon_{if}$ is the energy difference between discrete initial and final states. In evalu-

ating Eq. (2) we have described the hole continuum states by two-dimensional (2D) plane-wave states of momentum \mathbf{k} . The total Auger rate is obtained by summing over all hole levels laying above the minimum energy. Setting $f_h^j = 1$ in Eq. (2) gives an Auger rate of the order 1 ps^{-1} . The radiative recombination rate is given by

$$\Gamma_{rad}^{i \rightarrow j} = \frac{2\pi}{\hbar} \sum_{\mathbf{q}} |\langle \phi_e^i | \mathbf{d} \cdot \hat{\mathbf{E}} | \phi_h^j \rangle|^2 f_h^j \delta(\Delta \epsilon_{ij} - \hbar \omega_{\mathbf{q}}), \quad (3)$$

where i and j are the electron and hole states, respectively. The matrix element is implicitly assumed to be taken between the vacuum and the one-photon state \mathbf{q} . The electron and hole wave functions are nearly those of a 2D harmonic oscillator. For the radiative electron-hole recombination the selection rules are $\Delta n = 0$ and $\Delta m = 0$, where n is the radial and m the angular quantum number.¹⁶ Evaluating Eq. (3), gives an electron-hole recombination time of $\Gamma_{rad}^{-1} = 0.7 \text{ ns}$. This recombination time is nearly constant for the lowest laying QD levels. The angular quantum number m leads to a $d_i = 2m + 1$ -fold degeneracy of level i . Summing over the degenerate states, and setting the radiative and Auger matrix elements equal for all transitions, the master equation for the electrons becomes

$$\begin{aligned} \dot{u}^e(n_1 \dots) = & -\Gamma_p(t) \sum_i (d_i - n_i) u^e(n_1 \dots) \\ & + \Gamma_p(t) \sum_i (d_i - n_i + 1) u^e(n_1 \dots n_i - 1 \dots) \\ & - \Gamma_{rad} \sum_i n_i f_h^i u^e(n_1 \dots) \\ & + \Gamma_{rad} \sum_i (n_i + 1) f_h^i u^e(n_1 \dots n_i + 1 \dots) \\ & - \Gamma^A \sum_{jk} n_k (d_j - n_j) f_h^k u^e(n_1 \dots) \\ & + \Gamma^A \sum_{jk} (n_k + 1) (d_j - n_j + 1) \\ & \times f_h^k u^e(n_1 \dots n_j - 1 \dots n_k + 1 \dots), \quad (4) \end{aligned}$$

where the n_i refers to the one particle states including spin. The degeneracy factor d_i does not include the spin, as the master equation cannot be spin separated.

To obtain the hole populations, we sum over the electron degrees of freedom. The resulting equation will give the hole population probability, which then can be used to calculate the expectation value f_h^i . Three processes change the hole populations: LA-phonon emission/absorption, Auger emission (a redistribution of the electrons lead to an emission of a hole into the continuum), and hole capture from the QW. The LA-phonon rate is much slower than the other processes involved. It will therefore be the LA-phonon rate that determines how fast the hole population will thermalize. Direct calculations show that the time required for $f_h^i \rightarrow f_{therm}^i$ is on the order of 50–200 ps, depending on the temperature (higher temperature, faster thermalization). We make the assumption that the number of electrons in the QD equals the

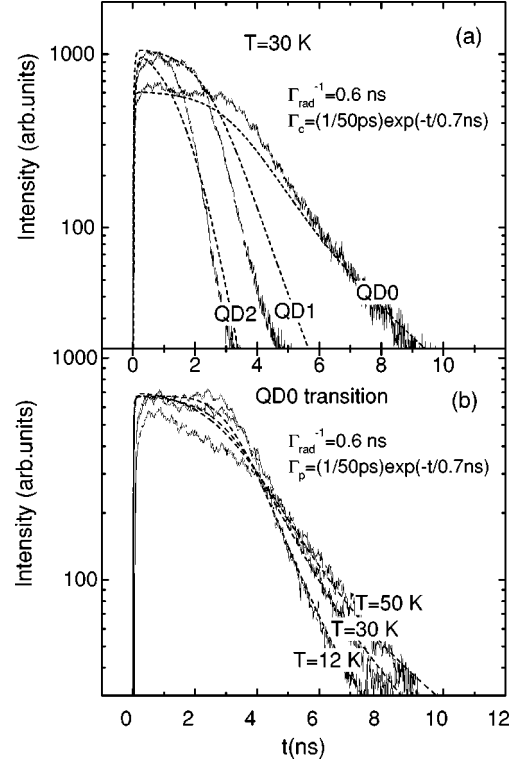


FIG. 3. A comparison of the computed time dependence of the intensities with the experimental data. In (a) we show the lines QD0, QD1, and QD2 at $T=30 \text{ K}$. In (b) the intensity of QD0 line is plotted as a function of time for temperatures of 12, 30, and 50 K.

number of holes. This assumption is based on the fact that the sample is initially neutral (or only very weakly positively doped), and that the absorption of photons creates electrons and holes in pairs. A situation where we would have a net charged QD would be energetically unfavorable due to Coulomb repulsion, so fluctuations in the net charge are suppressed. All excitonic effects have been excluded since it has been found that the independent particle picture is in good agreement with the observed state filling¹² and magnetoluminescence data.¹⁶

In numerically solving Eq. (4), we have included three QD levels, leading to a maximum system size of 12 electrons and 12 holes. Calculations on a QD with four electron levels, show that the inclusion of further levels, while greatly adding to the computational time, does not change the results in an essential way. Initially, the electrons (and holes) are in the QW. Luminescence rise-time measurements give rise times on the order of 1 ps.¹³ In our calculations Γ_0 controls the degree of state filling and thus relative ordering of the maximum intensity for the different QD lines. Experiments done at different excitation intensities (1–10 mW) show no change in the relative ordering of the QD lines. Our model is also quite insensitive to small changes in Γ_0 within this range. A best fit to experiment for a homogeneous excitation gives $\Gamma_0^{-1} = 50 \text{ ps}$ [Fig. 3(a)], whereas for a Gaussian profile we obtain $\Gamma_0^{-1} \approx 1 \text{ ps}$. The time constant τ_0 determines the length of the plateau region of the luminescence maximum [Fig. 3(a)]. The value of τ_0 is related to the decay time of the QW luminescence. The decay time 0.5 ns for the QW luminescence obtained from Fig. 1 is close to the fitted value $\tau_0 = 0.7 \text{ ns}$.

All lower, vacant electron states will be quickly filled by the Coulomb scattering from the QW and the Auger process. When 10 electrons and holes are present in the QD, the pure Auger rate at 12 K is approximately 0.5 ps^{-1} and at 50 K, 1 ps^{-1} . The situation changes drastically when only one electron and hole is left in the QD, where the corresponding rates are 1 ns^{-1} and 100 ns^{-1} , respectively, thus showing a prominent temperature effect. Note that these numbers depend critically on the depths of the confinement potentials. When the lower states are completely filled the Auger process will stop. Holes emitted will then be recaptured into the QD, where they are thermalized by the LA phonons. All this happens on a time scale that is much shorter than the radiative recombination time. The electrons will see a thermal hole population during the later stages of the carrier relaxation. Note that in our model the relaxation process is coupled to the hole population dynamics and therefore we cannot use a single constant rate to describe intraband relaxation.

A consequence of the thermal hole population is that the slope of the ground-state luminescence line QD0 (after the signal from the excited states has died away), is proportional to $\Gamma_{rad} f_h^i$, with $f_h^i = f_{therm}^i$. The slope is thus temperature dependent through the Fermi distribution of the holes. As f_{therm}^i is determined when we fix the temperature and the level spacing, a direct fitting of the experimental data gives $\Gamma_{rad}^{-1} = 0.6 \text{ ns}$, which is in excellent agreement with the theoretically calculated value of 0.65 ns [Fig. 3(b)]. The excited QD lines [not shown in Fig. 3(b)], have a very similar temperature behavior to the QD0 line, and also give a good agreement between theory and experiment. The increase in the QD luminescence relaxation time with increasing temperature is due to the thermal excitation of holes from the

lowest QD levels, thus leaving fewer holes for the electrons to recombine with. Further support for this interpretation is given by an experiment done on a QD sample where the QD hole level spacing is increased from 3 to 5 meV. For this sample the observed changes in the QD luminescence decay time as function of temperature are smaller, as predicted by our model. This trend is also consistent with experiments done on QD samples with much larger intersublevel energy spacing than our QD's. In these experiments a temperature-independent QD luminescence decay time is observed until the onset of thermionic emission of carriers from the QD.¹⁷ Thus if the intersublevel spacing is much larger than the thermal energy kT , the temperature dependence of the QD luminescence is expected to vanish. In calculating Fig. 3(b) we have fixed the value of the relaxation parameters at one temperature and the other luminescence curves has been produced by only varying the temperature. As can be seen from Figs. 3(a) and 3(b), there is not a perfect fit between theory and experiment at early stages when the number of carriers in the QD is large. It could be conjectured that the difference arises due to many-body effects, although this suggestion would need further work in order to be confirmed.

In conclusion we have presented a mechanism for breaking the phonon bottleneck, which gives a qualitative agreement with the measured luminescence. The observed temperature dependence of the time-resolved luminescence can be well explained by using the assumption of a thermal hole population.

The financial support of the Academy of Finland under Contracts Nos. 37787, 37789, 34158, and TEKES under Contract Nos. 537/401/96 is gratefully acknowledged.

-
- ¹U. Bockelmann and G. Bastard, *Phys. Rev. B* **42**, 8947 (1990).
²H. Benisty, C.M. Sotomayor-Torres, and C. Weisbuch, *Phys. Rev. B* **44**, 10 945 (1991).
³B. Ohnesorge *et al.*, *Phys. Rev. B* **54**, 11 532 (1996).
⁴V.I. Klimov and D.W. McBranch, *Phys. Rev. Lett.* **80**, 4028 (1998).
⁵S. Grosse *et al.*, *Phys. Rev. B* **55**, 4473 (1997).
⁶T.H. Gfroerer *et al.*, *Phys. Rev. B* **53**, 16 474 (1996).
⁷U. Bockelmann and T. Egeler, *Phys. Rev. B* **46**, 15 574 (1992).
⁸A.I.L. Efros, V.A. Karchenko, and M. Rosen, *Solid State Commun.* **93**, 281 (1995).
⁹P.C. Sercel, *Phys. Rev. B* **51**, 14 532 (1995).
¹⁰M. Sopianen, H. Lipsanen, and J. Ahopelto, *Appl. Phys. Lett.* **66**, 2364 (1995).
¹¹J. Tulkki and A. Heinämäki, *Phys. Rev. B* **52**, 8239 (1995).
¹²H. Lipsanen, M. Sopianen, and J. Ahopelto, *Phys. Rev. B* **51**, 13 868 (1995). Intensity distribution of cw luminescence has been analyzed in H. Lipsanen, M. Sopianen, and J. Tulkki, *The Optics of Semiconductor Wires and Dots*, edited by G. Bryant (Gordon and Breach, New York, in press), Vol. 8.
¹³J.H.H. Sandmann *et al.*, *Phys. Status Solidi A* **164**, 421 (1997).
¹⁴M. Braskén, M. Lindberg, and J. Tulkki, *Phys. Status Solidi A* **164**, 427 (1997).
¹⁵M. Grundmann and D. Bimberg, *Phys. Rev. B* **55**, 9740 (1997).
¹⁶M. Braskén, M. Lindberg, and J. Tulkki, *Phys. Rev. B* **55**, 9275 (1997).
¹⁷G. Wang *et al.*, *Appl. Phys. Lett.* **64**, 2815 (1994); K. Mukai *et al.*, *Phys. Rev. B* **54**, R5243 (1996); S. Fafard *et al.*, *Surf. Sci.* **361**, 778 (1996); S. Raymond *et al.*, *Can. J. Phys.* **74**, S216 (1996); J. Arlett *et al.*, *J. Vac. Sci. Technol. B* **B16**, 578 (1998).